EXTRACTING VEGETATIONAL FEATURES FROM LANDSAT MAPS: USING A DELAY AND SUM BEAMFORMING FOR IMAGE PROCESSING

A. Lay-Ekuakille[1], D.P. Bakajika Mukombo[2], John P. Djungha Okitadiowo[3] A. Nyengele[4], C. Lefi[5], C. Ntuala Ompua[6], M. Palmisano[7]

[1] University of Salento, Dept of Innovation Engineering, Lecce, Italy, aime.lay.ekuakille@unisalento.it
[2] UPN University, ETS School, Dept of Telecommunications, Kinshasa, DR Congo, derrickbakajika96@gmail.com
[3] University of Reggio Calabria, Dept of Information Engineering, Reggio Calabria, Italy, johnpdjungha@unirc.it
[4] UPN University, ETS School, Dept of Geomatics, Kinshasa, DR Congo, dorismubenga@gmail.com
[5] ISTA University, Dept of Mechanics, DR Congo, dechris.lefi@gmail.com
[6]Congo Futur, Kinshasa, Kinshasa, DR Congo, christellecno@gmail.com
[7]National Research Council, ISAFOM, Benvento, Italy, maurizio.palmisano@cnr.it

Abstract:
Remote sensing has been performing a robust help in addressing issues related to extract information from satellite, and airborne-based platforms. This extraction is certainly a way for making quality and quantity analysis, hence measurements. This paper intends to illustrate the application of the delay and sum beamforming (DSB) approach to characterize satellite maps, in particular Landsat ones, for classifying different soil/land characteristics. The algorithm has been tested to detect the vegetation index from Lansat images of the city of Kinshasa (DR Congo). The DSB has demonstrated to exhibit better results than traditional techniques because of its accurate and reliable results.

Keywords: NDVI, Delay and sum beamforming, Environmental measurements, Forestation, Environmental economy, Remote sensing, Landsat

1. INTRODUCTION

All techniques for evaluating the effects of land use changes on landscape are based on the efficient use of land use/land cover datasets. So, the first operation in most cases is based on the choice or elaboration of geodatabases that collect land use data. Currently, this task is simpler than in the past thanks the progressive increase of freely available multi-source geodata, which allows a detailed reconstruction - and for large time periods - of land use changes [1]. Furthermore, another fundamental assumption is represented by the use of GIS tools, which allows the application of different methodologies for the evaluation of landscape dynamics; both those are based on historical approaches and on the use of remote sensing or on an integrated approach between these different techniques.

Landsat is currently nearing five decades of uninterrupted satellite imaging [2]. The

initiation of the Landsat program was in 1972, providing for some locations an early baseline for change detection that is unique among satellite programs [3]. Later changes to the Landsat data policy in 2008 by the United States Geological Survey (USGS) resulted in free and open access to the global Landsat archive [4]. This policy change lead to a vast increase in global applications, particularly in terms of monitoring changes over large areas [5] and to the formalization of Landsat data in commercial and government programs [6]. Efforts have been made by the Landsat Global Archive Consolidation (LGAC) to ensure that all images gathered at international receiving stations are captured, processed, stored, and made available via the collection of Landsat data into the USGS Landsat data archive. Today, the Landsat archive is more complete than ever [7].
As indicator, better one of the most known the NDVI (normalized difference vegetation index) is one of the most known metrics. It is computed according to formula reported in Eq.1, that is

$$NDVI = \frac{NIR - RED}{NIR + RED} \tag{1}$$

in which NIR is the reflection in the near-infrared spectrum, and RED is the reflection in the red range of spectrum. We can directly apply the above formula in the case of the example reported in Fig.1. For the healthy tree it is 0,69 whilst for the stressed one, it is 0,006. The range 0.60-0.80 is typically connected to temperate and tropical rainforests. The increasing of the NDVI is a good thing for preserving trees, hence vegetation from degradation.

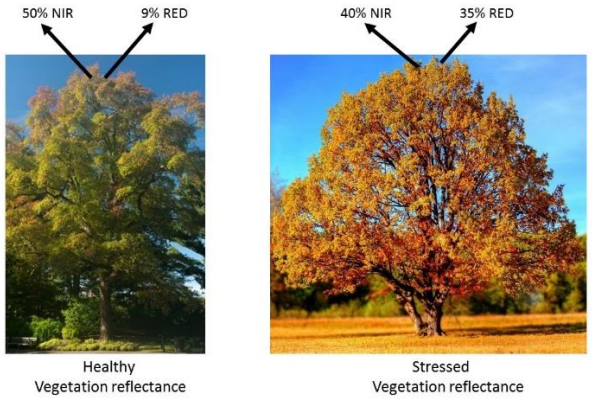

Figure 1: NDVI impact on vegetation health

Sometimes, it could be difficult to process images in order to obtain reliable NDVI because of noise included in the data. A further processing of these images could be necessary. There are different techniques to process them. Here we propose one based on a beamforming approach.

2. STUDY AREA

The study area is the big city of Kinshasa, the capital of the Democratic Republic of Congo, displaying an extension around 9,965 km^2 (square km), with around 12 million of inhabitants. Only 600 km^2 of the territory is densely crowded. The remaining part of the territory is covered and occupied by woods, rivers, savannah, and bare soil. However, Kinshasa has been undergoing a high pressure of expansion and extension due to the quick increasing of inhabitants.

Fig. 2 illustrates the overview map, retrieved from Landsat satellite, displaying the NDVI values in the city of Kinshasa. The red points and areas are densely subject to human activities. There is a massive activity of reducing woods and rainforests that bring to frequent and regular landslides, floods, and soil resilience losses. The woods are preserved along the inner rivers, streams, and waterways.

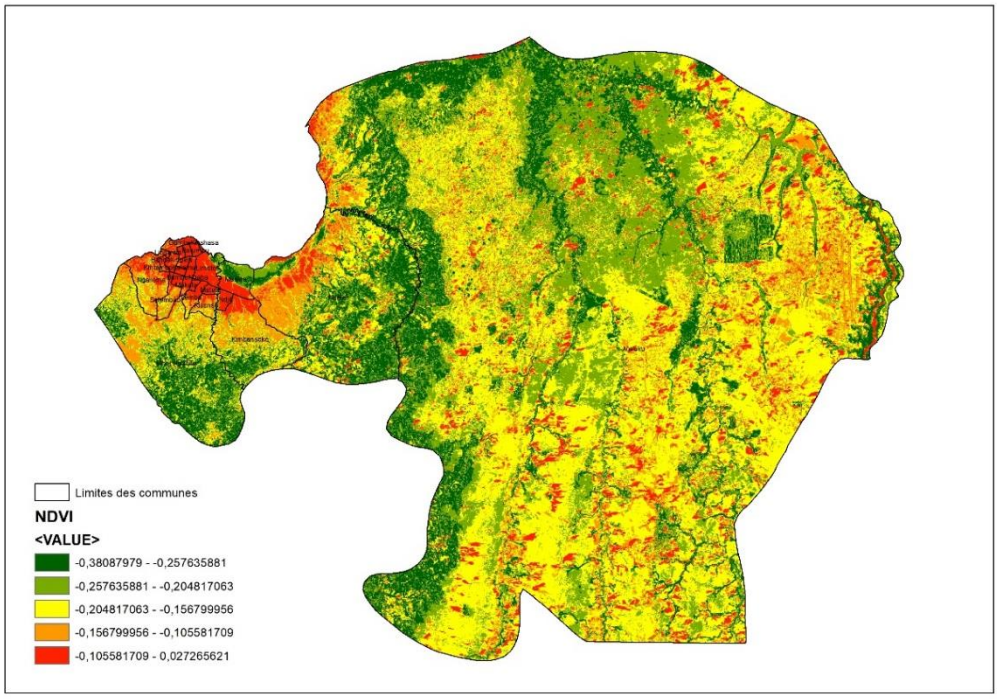

Figure 2: Distribution of concentration

Moreover, the study regarding the vegetation condition is an important asset with high impact on the economy. The trees, the woods and the forests are basically the resources that can regulate the economy of a country. In particular for tropical areas, they assume a specific role for the following main reasons: (i) wood for cooking; (ii) local construction, housing, and furniture; (iii) exportation for foreign needs; (iv) environmental protection for local and global interests.

Recalling the climate change, major increases in human activities over the last century have resulted in forest decline, particularly in the tropical areas of the world. Forest decline manifests as both deforestation—that is, depletion of the tree crown cover to less than 10 percent, and degradation, or negative structural or functional changes that reduce forest quality (e.g. through over-exploitation, repeated fires, or disease) [8].

3. BEAMFORMING APPROACH FOR IMPROVING QUALITY OF NDVI

In forestry applications, estimating 3D reflectivity is very important for mapping forest structure, in terms of the spatial distribution of canopy layers that could be estimated from reflectivity profiles. Therefore, the performance of a given reconstruction algorithm to reflect the variability of forest structure must take into account its ability to unambiguously detect the presence of a forest layer while remaining invariant to non-structural changes. This implies resolution, but also the ability to reflect weak scatterers.

During this research we experimented with Tomographic SAR Inversion with the Dual polarimetric Beamforming (DPB) [9] algorithm to try to extract mapping from a SAR image, there are other techniques, methods and algorithms such as Capon Beamforming and compressive sensing (CS) as well as radiometric accuracy, stability, MUSIC [10], LMS and polarimetric accuracy. When TomoSAR acquisition is performed, tomographic processing techniques will now be required to extract 3D reflective mapping from the scene, so there are many methods for reconstructing the topography of the image of a photographed area from TomoSAR data that exist, many of which we have mentioned above. These methods all have different behaviour and performance depending on the characteristics of the scene and the acquisition parameters of the system. Thus, the linear reconstruction by the DP-Beamforming method optimises the processing of the imagery, based on the minimisation of the variance at each height, and is widely used and tested in forestry scenarios. Allowing the achievement of a nice resolution and reducing side lobes, with an exploitation of the underlying structure of the data and which manages to solve the big convex optimization problem. It is also very important to point out that the performance of DP-Beamforming is less and less sensitive to non-uniform distributions.

Beamforming [11], also known as spatial filtering, beamforming or channel forming, is a signal processing technique used in antenna and sensor arrays for the directional transmission or reception of signals. This is achieved by combining the elements of a phased array antenna in such a way that directions the signals interfere constructively while in other directions the interference is destructive.

Beamforming can be used at the transmitter or receiver end to achieve spatial selectivity. The improvement, compared to the transmission/reception of an isotropic (omnidirectional) antenna, is called the transmission/reception gain (or loss). It is very important to point out that beamforming algorithms can process images and videos very well, apart from its advantage on signal processing and transmission.

We used the dual polarimetric Beamforming algorithm [12] to focus the topography on the same geographic coordinate system of the study region. Today Beamforming is becoming the most common spectral estimation algorithm in the field of Synthetic Aperture Radar Surveying. The ordinary Beamforming is so considered as finite state impulse response filter, so this filter will give the signal a certain spatial frequency to pass without distortion which allows to attenuate the signal from other frequencies. The classical algorithm of Beamforming the dual polarimetric Beamforming estimator is demonstrated in the way. The optimization of dual polarimetric Beamforming is given by:

$$\frac{\min h}{h}\frac{H}{B}h_B s.t. h_B^H a(z_d,k_d)=1 \tag{2}$$

N is image in DP mode, and where h_B represents the filter of the DP-beamforming algorithm which has the following expression

$$h_B=\frac{a(z_d,k_d)}{a^H(z_d,k_d)a(z_d,k_d)}=\frac{a(z_d,k_d)}{N} \tag{3}$$

z_d, k_d are considered as vectors, the signal after filtering has this power:

$$E\left\{\beta_D(i)\beta_D^H(i)\right\}=\frac{a^H(z_d,k_d)R_a(z_d,k_d)}{N^2} \tag{4}$$

It could be maximised depending on the polarisation state k_d by:

$$\max_{\|k_d\|_2=1}\frac{a^H(z_d,k_d)R_a\dfrac{a^H(z_d,k_d)}{N^2}}{N^2} \tag{5}$$

where R is considered as the covariance matrix of the DP-Tomography Synthetic aperture radar model. On the reduction of the calculations, the direction vectors a z_d, k_d must be written as such:

$$a(z_d,k_d)=(I_{(2\times2)}\otimes(z_d)k_d=B(z_d)k_d \tag{6}$$

That is, the maximum problem in equation 4 could become a maximum eigenvalue problem of the Hermitian matrix that is B:

$$B^H(z_d)RB(z_d)K_{d\max} = \lambda_{\max}k_{\max} \quad (7)$$

K is the polarization measurement vector of two different polarization channels.

In conclusion the power of DP-Beamforming is delivered:

$$\hat{P}_{BP(z_d)} = \frac{\lambda_{\max}\left(B^H(z_d)\hat{R}_{DP(z_d)}\right)}{N^2} \quad (8)$$

where $\lambda_{\max}$ denotes the maximum eigenvalue of the positive semidefinite matrix.

$$\hat{R}_{DP} = \frac{1}{L}\sum_{i=1}^{L} G_{DP}(i)G_{DP}^H(i) \quad (9)$$

$\hat{R}_{DP}$ represents the matrix of vectors, which can be obtained after decomposing the eigenvalues of the sample covariance matrix [13]. The above formulation will bring to the topological map.

We have used the LMS (Least Mean Squares) beamforming to improve the images previously treated with other techniques such as ENVI, Erdas Imagine, Idrisi, ArcGIS, MapInfo. In a clear way, thE post-processing is necessary to improve the quality of the images processed by traditional way. The algorithm depicted in Fig.3 is used for determining the new NDVI after processing.

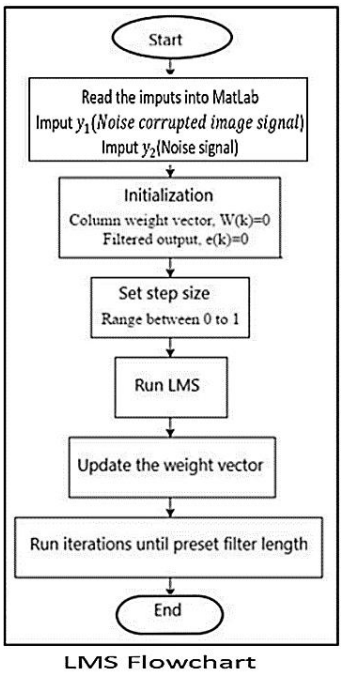

Figure 3: LMS Beamforming

4. RESULTS AND DISCUSSION

Fig.4 exhibits the results as outcomes of GIS (Geografic Information System) processing. As we can see, despite the overlapping of two different bands of Landsat, that is band 4 and band 5, th results are difficult to be interpreted because they are fair, and we need a further processing as demonstrated forward. Prior to the explanation, we need to understand the role of each band in Landsat imaging. The sensors aboard each of the Landsat satellites are designed to acquire data in different ranges of frequencies along the electromagnetic spectrum (see Table I as example). The Multispectral Scanner (MSS) carried on Landsat 1,2,3,4 and 5 collected data in four ranges (bands); the Thematic Mapper (TM) sensor on Landsat 4 and Landsat 5 included those found on earlier satellites and also introduced a thermal and a shortwave infrared band. A panchromatic band was added to Landsat 7's Enhanced Thematic Mapper Plus (ETM+) sensor.

Table I. Properties of some Landsat bands

Band	**Wavelength** (μm)	**Useful for mapping**
Band 4 - Near Infrared	0.64-0.67	Emphasizes biomass content and shorelines
Band 5 - Short-wave Infrared	0.85-0.88	Discriminates moisture content of soil and vegetation; penetrates thin clouds

These two images, of band 4 and band 5, are from Landsat 8 with their resolution of 30 meters. Certainly, it is a good resolution but band 4 and band 5 works in red and near infrared respectively. The areas taken into consideration are encompassed in the districts of Maluku, N'sele, Kisenso, and Mont-Ngafula, all in Kinshasa. It was necessary to point out them before post-processing by using the topological approach by means of dual polarimetric beamforming, as reported in Fig.5.

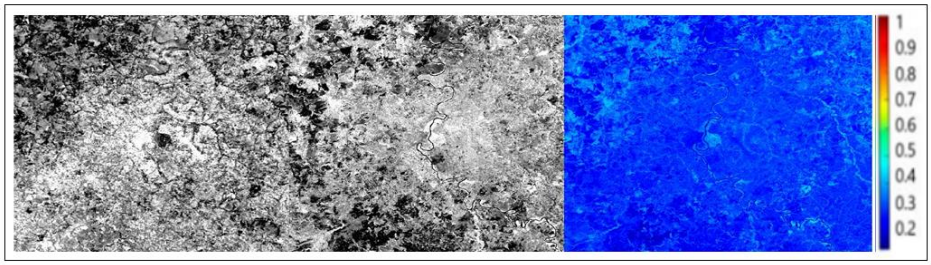

Figure 4: Landsat images: band 4 (left), band 5 (center), and calculated NDVI (right)

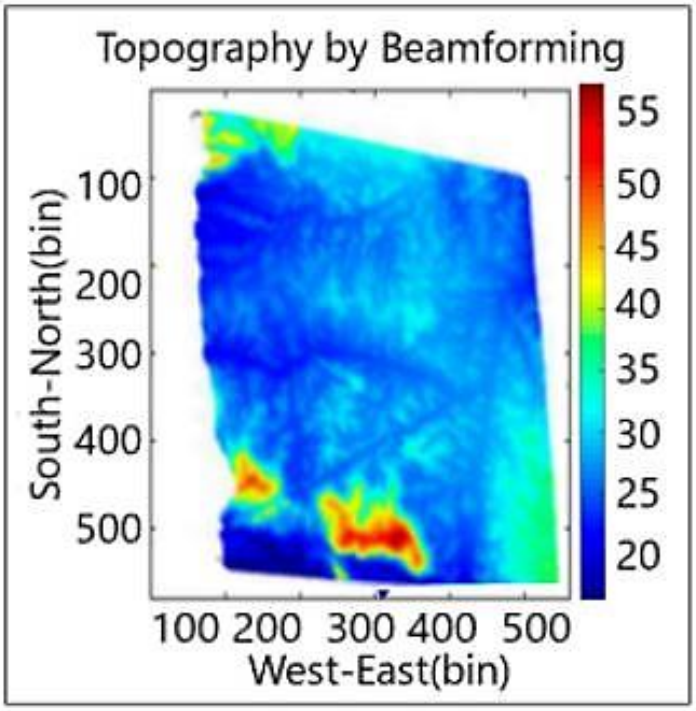

Figure 5: Implemented DP beamforming-based topography using Landsat images

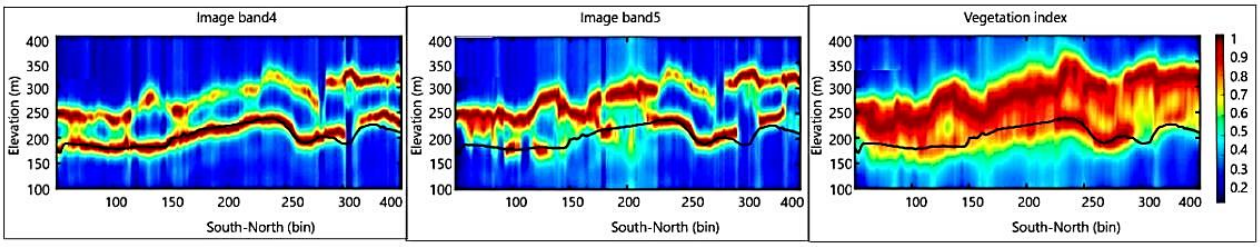

Figure 6: Reprocessed maps using Least Mean Squares Beamforming including NDVI

The post-processing has been performed by means of the LMS beamforming. This latter works as spatial filtering trying to process information contained in a signal from diverse sources. The LM beamforming better exploits the Landsat 8 operational Land Imager (OLI) and Thermal Infrared Sensor (TIRS) images that consist of nine spectral bands with a spatial resolution of 30 meters for Bands 1 to 7 and 9. New band 1 (ultra-blue) is useful for coastal and aerosol studies. New band 9 is useful for cirrus cloud detection. The resolution for Band 8 (panchromatic) is 15 meters. Thermal bands 10 and 11 are useful in providing more accurate surface temperatures and are collected at 100 meters. Working in band 4 and 5, that is red and infrared, we are able to detect the necessary information in order to apply the Eq. (1), as reported in the first section of this paper. Fig.6 finally shows the results of using LMS Beamforming in both bands, and it is possible to observe the efficiency of the LMS beamforming in detecting the different areas by targeting the

points where the NDVI is minimum, that is the red colour.

As we can see in Fig. 6 the colour work of the LMS algorithm, detailed as follows: the blue colour represents areas with stable and prosperous vegetation, the yellow colour represents unstable vegetation that is not prosperous, and finally we have the red colour that clearly shows areas with advanced deforestation.

5. CONCLUSIONS

The paper has illustrated the application of a beamforming algorithm for better post-processing GIS treatments in aspecific areas. Clearly, we can say that the LMS beamforming results give more precision, as we detailed in the last paragraph of the results and discussion section.

LMS beamforming detects the different sources in red and near infrared bands, as we can see on Fig. 4.

The proposed algorithm is more accurate than GIS one. Certainly, the significant discrepancy between both analysis is due to the complexity of the targeted land [14]. The beamforming can be more accurate.

6. REFERENCES

[1] G. Cillis, A. Lay-Ekuakille, V. Telesca, D. Statuto, P. Picuno, "Analysis of the Evolution of a Rural Landscape by Combining SAR Geodata with GIS Techniques", International Mid-Term Conference 2019 of the Italian Association of Agricultural Engineering (AIIA), pp.255-263, September 12-13, 209, Matera, Italy.

[2] W.B. Meyer, H. Turner, "Human Population Growth and Global Land-Use/Cover Change. Annu. Rev. Ecol. Syst. Vol.23, pp.39–61, 1992.

[3] A.S. Belward, J.O. Skøien, "Who Launched What, When and Why; Trends in Global Land-Cover Observation Capacity from Civilian Earth Observation Satellites", ISPRS J. Photogramm. Remote Sens. Vol.103, pp. 115–128, 2015.

[4] C.E. Woodcock, R. Allen, M. Anderson, A. Belward, R. Bindschadler, W. Cohen, F. Gao, S.N. Goward, D. Helder, E. Helmer, et al., "Free Access to Landsat Imagery, Science, Vol. 320, 101, 2008.

[5] M.A. Wulder, J.G. Masek, W.B. Cohen, T.R. Loveland, C.E. Woodcock, "Opening the Archive: How Free Data Has Enabled the Science and Monitoring Promise of Landsat", Remote Sens. Environ. Vol.122, pp. 2–10, 2012.

[6] Z. Zhu, M.A. Wulder, D.P. Roy, C.E. Woodcock, M.C. Hansen, V.C. Radeloff, S.P. Healey, C. Schaaf, P. Hostert, P. Strobl, et al., "Benefits of the Free and Open Landsat Data Policy", Remote Sens. Environ. 224, 382–385, 2019.

[7] M.A. Wulder, J.C. White, T.R. Loveland, C.E. Woodcock, A.S. Belward, W.B. Cohen, E.A. Fosnight, J. Shaw, J.G. Masek, D.P. Roy, "The Global Landsat Archive: Status, Consolidation, and Direction", Remote Sens. Environ. Vol. 185, pp.271–283, 2016.

[8] J. C. Cuaresma, O. Danylo, S. Fritz, I. McCallum, M. Obersteiner, L. See, B. Walsh, Economic Development and Forest Cover: Evidence from Satellite Data, Scientific reports, 7:40678 | DOI: 10.1038/srep40678

[9] S. Sauer, L. Ferro-Famil, A. Reigber, E. Pottier, "Three-Dimensional Imaging and Scattering Mechanism Estimation over Urban Scenes Using Dual-Baseline Polarimetric InSAR Observations at L-Band", IEEE Trans. Geosci. Remote Sens. Vol.49, pp.4616–4629, 2011.

[10] P. Vergallo, A. Lay-Ekuakille, Brain Source Localization: A New Method Based On Music Algorithm and Spatial Sparsity, Rev. Sci. Instrum. 84, 085117, 2013.

[11] A. Lay-Ekuakille, P. Vergallo, D. Saracino, A. Trotta, Optimizing and Post Processing of a Smart Beamformer for Obstacle Retrieval, IEEE Sensors Journal, vol.12, issue 5, pp.1294-1299, 2012.

[12] H. Aghababaee, M.R. Sahebi, "Model-Based Target Scattering of Polarimetric SAR Tomography", IEEE Trans. Geosci. Remote Sens. 2018, 56, 972–983.

[13] L. Ferro-Famil, Y. Huang, E. Pottier, "Principles and Applications of Polarimetric SAR Tomography for the Characterization of Complex Environments", In VIII Hotine-Marussi Symposium on Mathematical Geodesy; Springer: Cham, Switzerland, pp. 243–255, 2015.

[14] A. Lay Ekuakille, F. Tralli, M. Tropeano, (2000), Land Modification Measurements Using ERS-2 Satellite Images, XVI IMEKO World Congress, Vienna, Austria, September 25-28, 2000